ORIGINAL INVESTIGATION

Multi-modal antidepressant-like action of 6- and 7-chloro-2-aminodihydroquinazolines in the mouse tail suspension test

Kavita A. Iyer[1] · Katie Alix[1] · Jose M. Eltit[2] · Ernesto Solis Jr.[2] · Xiaolei Pan[3] · Malaika D. Argade[1] · Shailesh Khatri[4] · Louis J. De Felice[2] · Douglas H. Sweet[3] · Marvin K. Schulte[5] · Małgorzata Dukat[1]

Abstract

Rationale 2-Amino-6-chloro-3,4-dihydroquinazoline (e.g., A6CDQ) represents a novel putative antidepressant originally thought to act through a 5-HT$_3$ serotonin receptor antagonist mechanism. Here, we investigated this further by examining a positional isomer of A6CDQ (i.e., A7CDQ).

Materials and methods 5-HT$_3$ receptor and transporter activity (uptake-1 and uptake-2) were investigated using a variety of in vitro assays and the in vivo mouse tail suspension test (TST).

Results Although A7CDQ binds at 5-HT$_3$ receptors with low affinity ($K_i = 1975$ nM) compared to A6CDQ ($K_i = 80$ nM), it retained 5-HT$_3$ receptor antagonist action (IC$_{50} = 5.77$ and 0.26 μM, respectively). In the mouse TST A7CDQ produced antidepressant-like actions (ED$_{50} = 0.09$ mg/kg) comparable to that of A6CDQ. In addition, A6CDQ was found to be a 5-HT releasing agent ($K_m = 2.8$ μM) at hSERT and a reuptake inhibitor (IC$_{50} = 1.8$ μM) at hNET, whereas A7CDQ was a weak reuptake inhibitor ($K_m = 43.6$ μM) at SERT but a releasing agent (EC$_{50} = 3.3$ μM) at hNET. Moreover, A6CDQ and A7CDQ were potent inhibitors of uptake-2 (e.g.; OCT3 IC$_{50} = 3.9$ and 5.9 μM, respectively).

Conclusions A simple shift of a substituent in a common quinazoline scaffold from one position to another (i.e., a chloro group from the 6- to the 7-position) resulted in a common action in the TST but via a somewhat different mechanism. A6CDQ and A7CDQ might represent the first members of a new class of potential antidepressants with a unique multi-modal mechanism of action.

Keywords 5-HT$_3$ receptors · Uptake-1 · Uptake-2 · SERT · NET · OCT · Electrophysiology · TST · Mice

De Felice is deceased

✉ Małgorzata Dukat
mdukat@vcu.edu

1 Department of Medicinal Chemistry, School of Pharmacy, Virginia Commonwealth University, PO Box 980540, Richmond, VA 23298-540, USA

2 Department of Physiology and Biophysics, School of Medicine, Virginia Commonwealth University, Richmond, VA 23298, USA

3 Department of Pharmaceutics, School of Pharmacy, Virginia Commonwealth University, Richmond, VA 23298, USA

4 Department of Pharmaceutical Sciences, Philadelphia College of Pharmacy, University of Sciences, Philadelphia, PA 19104, USA

5 Department of Biomedical and Pharmaceutical Sciences, College of Pharmacy, Kasiska Division of Health Sciences, Idaho State University, Pocatello, ID 83209, USA

Introduction

Depression is a common illness affecting > 300 million people worldwide (WHO 2018). The World Health Organization reports that depression is the most prevalent cause of illness-induced disability with a significant economic burden (WHO 2018). Current antidepressant treatments such as tricyclic antidepressants (TCAs) and selective serotonin reuptake inhibitors (SSRIs) appear to be effective only in approximately half of patients, leaving nearly 50% of patients refractory to current treatments (Daws et al. 2013). Therefore, there is a growing need for mechanistically novel antidepressants.

A low synaptic concentration of the neurotransmitters serotonin (5-HT) and norepinephrine (NE) (Fig. 1) is one of the simplest and most commonly accepted hypotheses of depression (Carlsson et al. 1969), and agents that increase synaptic concentrations of 5-HT and NE are seen as therapeutically
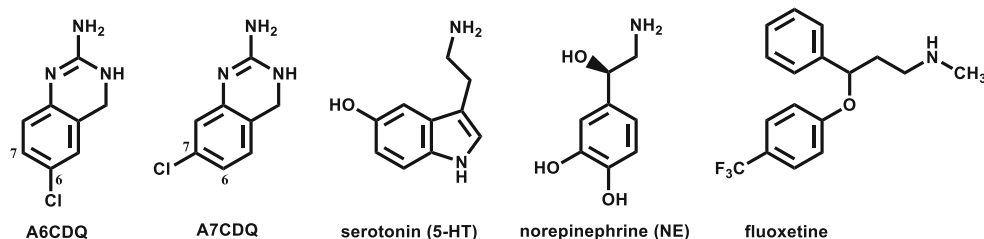
Fig. 1 Chemical structures of 2-amino-6-chloro-3,4-dihydroquinazoline (A6CDQ) and its positional isomer 2-amino-7-chloro-3,4-dihydroquinazoline (A7CDQ) showing dissimilarity with 5-HT, NE, and fluoxetine

promising agents. This increase might involve one of several different aminergic mechanisms. For example, fluoxetine (Fig. 1), one of the first SSRIs and a widely prescribed antidepressant (Andersen et al. 2014), targets and binds to the serotonin transporter (SERT) with high affinity ($K_i = 1$ nM) (Andersen et al. 2014) to block transporter-mediated recapture of 5-HT from the synapse (Rothman and Baumann 2003). A mechanistically different class of xenobiotics, substrate-type releasers, target transporter proteins and promote efflux via a transport-mediated exchange process (Rothman and Baumann 2003). Nichols and co-workers have previously examined SERT releasers (i.e., 5-methoxy-6-methyl-2-aminoindan (MIMAI) and p-methylthioamphetamine (MTA)) in animal behavioral studies as potential antidepressants (Marona-Lewicka and Nichols 1997; Scorza et al. 1999). A limited number of clinical studies suggest that 5-HT releasing agents might have a beneficial effect in patients suffering from certain types of depression (for review see: Rothman and Baumann 2002).

In addition to sodium- and chloride-coupled "uptake-1"—high-affinity, low-capacity biogenic monoamine transporters SERT and NET (norepinephrine transporter)—there exists an ion-independent alternative uptake mechanism; "uptake-2"—low-affinity, high-capacity organic cation transporters (OCTs) contributing to clearance of aminergic neurotransmitters from the synapses (Daws et al. 2013). A high-capacity transporter (i.e., OCT3) limits the net increase of 5-HT and/or NE following therapeutic administration of an SSRI and/or SNRI (Daws et al. 2013). Thus, poor therapeutic responses to treatment with currently available antidepressants might be explained by "uptake-2".

Individual 5-HT receptor subtypes represent other targets for antidepressants. 5-HT₃ receptor antagonists have been demonstrated to produce antidepressant-like effects in several preclinical (i.e., rodent) models of depression (Ramamoorthy et al. 2008; Dukat et al. 2013). In addition, clinical studies show that some 5-HT₃ receptor antagonists (e.g., ondansetron, tropisetron) can relieve certain symptoms associated with depression (reviewed: Ramamoorthy and Radhakrishnan 2010 and Bétry et al. 2011). It has been suggested that inhibition of 5-HT₃ receptors facilitates both 5-HT and NE neurotransmission (Ramamoorthy and Radhakrishnan 2010; Perez-Palomar et al. 2018; respectively).

It is commonly held that fluoxetine's primary mechanism of antidepressant action involves inhibition at SERT; however, in addition to its SERT activity, fluoxetine allosterically inhibits 5-HT₃ receptor-mediated currents in rat neurons (reviewed: Davies 2011) and behaves as a functional antagonist at h5-HT₃A receptors (Table 1; Eisensamer et al. 2003). It has been proposed that fluoxetine's action at 5-HT₃ receptors contributes to its antidepressant effects (Ramamoorthy and Radhakrishnan 2010), and, moreover, SSRI-induced 5-HT elevation in the synapse leads to receptor desensitization reducing 5-HT₃ receptor activity (Bétry et al. 2011).

Previously, we demonstrated that 2-amino-6-chloro-3,4-dihydroquinazoline (A6CDQ; Fig. 1) possesses potent antidepressant-like activity in the mouse tail suspension test (TST), and is a potent 5-HT₃ receptor antagonist (Table 1), with nanomolar affinity ($K_i = 80$ nM). Conversely, it was described that A7CDQ (2-amino-7-chloro-3,4-dihydroquinazoline, Fig. 1), a positional isomer of A6CDQ, has low affinity at 5-HT₃ receptors, $K_i = 1975$ nM (Dukat et al. 2013).

In the present study, we examined the role of 5-HT₃ receptors on the antidepressant-like activity of both compounds comparing their action in the mouse tail suspension test. Unexpectedly, A7CDQ was found to be as potent as A6CDQ in this assay, ruling out 5-HT₃ receptors as the main common target responsible for their antidepressant-like activity. Using different expression systems, we studied other potential targets of these drugs that can contribute to their effects, and here we provide evidence that these dihydroquinazoline derivatives have multi-modal and concerted effects on

Table 1 Radioligand binding affinity data reported as K_i values (nM) and functional activity data EC_{50}, IC_{50} values for m5-HT₃A receptor (μM ± SE)

Ligands	5-HT₃[a]	5-HT₃A (EC_{50}/IC_{50})[b]
5-HT		2.20 ± 1.11
A6CDQ	80	0.26[a]
A7CDQ	1975	5.77 ± 1.13
Fluoxetine	> 10,000[c]	2.29[d]

[a] Previously reported (Dukat et al. 2013); [b] EC_{50} value for 5-HT; IC_{50} values for A6CDQ, A7CDQ, and fluoxetine; [c] Data taken as an average from the PDSP data bank; [d] Data from Eisensamer et al. 2003

monoaminergic uptake-1 and uptake-2 that can contribute to their antidepressant-like effects.

Materials and methods

In vitro 5-HT₃ functional studies: **Functional characterization in *Xenopus* oocytes—brief methodology** Ovarian lobes were surgically removed from *Xenopus laevis* frogs and washed twice in Ca^{2+}-free modified Barth's buffer (82.5 mM NaCl/2.5 mM KCl/1 mM $MgCl_2$/5 mM HEPES, pH 7.4). Lobes were gently shaken with 1.5 mg/mL collagenase (Sigma type II, Sigma–Aldrich) for 1 h at 20–25 °C. Stage IV oocytes were selected for microinjection. Synthetic cRNA encoding the m5-HT₃A receptor was prepared using mMACHINE™ High Yield Capped RNA Transcription Kit (Ambion, TX). Each oocyte was injected with 50 nL of cRNA at a concentration of 0.3 ng/nL. Oocytes were incubated at 19 °C for 2–4 days before conducting electrophysiological experiments. Electrical recordings were made using conventional two-electrode voltage clamp at − 60 mV employing an OC-725C oocyte clamp amplifier (Warner Instruments, CT, USA) coupled to an online, computerized data acquisition system (pCLAMP, Molecular Devices, LLC, USA).

The use of mouse receptors in functional studies permits a direct correlation between the functional effects of the receptor and the observed behavioral effects. However, there is significant similarity in both sequence and functional pharmacology of human and mouse 5-HT₃Rs; thus, the results of these studies would be directly transferable to human receptor interactions (Miyake et al. 1995; Hope et al. 1996). Mouse and human 5-HT₃Rs share approximately 91% sequence homology and are similar in their responsiveness to 5-HT. The EC_{50} for 5-HT on human receptors is 1.74 μM, comparable to the mouse receptor at 2.2 μM (Thompson and Lummis 2013; Dukat et al. 2013). Prior studies have shown small differences between human and mouse receptors, for example mCPBG displays higher affinity at rodent compared to human receptors, and 2 Me-5HT is a partial agonist at mouse receptors and a full agonist at human receptors (Miyake et al. 1995). However, the primary differences appear to be in the relative potency of ligands across species, not in receptor selectivity.

Recording and current electrodes were filled with 3 M KCl and had a resistance of 1–2 MΩ. Oocytes were held in a chamber with a volume of 280 μL and perfused with ND-96 recording buffer (96 mM NaCl/2 mM KCl/1.8 mM $CaCl_2$/1 mM $MgCl_2$/5 mM HEPES, pH 7.4). All test compounds were prepared in ND-96 buffer and applied at a rate of 20 mL/min using an automated Gilson 234 perfusion system.

In mock transfections of Xenopus oocytes, no currents were observed in response to 5-HT or other 5HT₃ receptor agonists. To determine if A7CDQ was capable of inducing currents (agonist action), oocytes expressing m5-HT₃A

receptors were exposed to the compound at increasing concentrations up to a maximum of 30 μM. As A7CDQ failed to induce currents, it was further evaluated for its ability to inhibit 5-HT-induced responses (antagonist action). Oocytes were first exposed to a concentration of 5-HT equal to the determined EC_{50} for 5-HT on these receptors (2.2 μM) to determine the uninhibited response amplitude. The same oocyte was then exposed to mixture of 2.2 μM 5-HT and increasing concentrations of A7CDQ (0.1 to 30 μM). Peak current amplitudes for each response were normalized to the uninhibited 2.2 μM 5-HT response. Concentration/normalized response curves were created and data were fit using a single-site competition model and GraphPad Prism (GraphPad Software Inc. La Jolla, CA).

Behavioral studies

Animals Male ICR mice (19–30 g) were used throughout the study (Harlan Laboratories, Indianapolis, IN). The current manuscript is a continuation of our previous studies with A6CDQ (Dukat et al. 2013) conducted using ICR mice as subjects. Thus, to make a direct comparison between the two positional isomers, A6CDQ and A7CDQ, we used ICR mice. ICR (CD-1) mice are the most widely used outbred mouse and the most economical. Moreover, Lucki (Lucki et al. 2001) investigated 11 strains of mice and showed that in the forced swimming test (another model of antidepressant-like activity), CD-1 mice were the second top (after the C57BL/6J) strain with a long duration (118 s) of immobility compared to other strains (e.g., NIH Swiss; 51 s) during the 6-min observation time in the absence of drugs.

Mice were housed in groups of 4–5 in solid-bottom plastic cages in a temperature (~ 22 °C)- and humidity (~ 50%)-controlled room. A standard 12:12 h dark:light cycle (light on at 0700 h) was used, and food and water were available ad lib. The experiments were conducted according to standards set by the Institutional Animal Care and Use Committee (IACUC) of the Virginia Commonwealth University and NIH Guide for Care and Use of Laboratory Animals. Mice were allowed to adapt to the testing environment for at least 1 h prior to any treatment, and weighed 30 min prior to the start of the experiments.

Drugs Fluoxetine hydrochloride (Prozac®, Batch 4A/80352; Eli Lilly) was purchased from Tocris, whereas imipramine hydrochloride (Tofranil®, Lot 27H1380; Novartis) was purchased from Sigma. Compounds A6CDQ and A7CDQ were previously synthesized in our laboratory (Dukat et al. 2013) and used as their HCl salts. Solutions were prepared fresh daily; all drugs were dissolved in 0.9% saline and administered to mice in a total volume of 10 mL/kg body weight by intraperitoneal (i.p.) injections.

Tail suspension test The TST, introduced by Steru (Steru et al. 1985) is a procedure inspired by Porsolt's Forced Swim Test (FST) (Porsolt et al. 1977) model for screening antidepressants in mice called "behavioral despair". The TST is based on the observation that normal mice exposed to aversive situations alternate between two behaviors: agitation and immobility. In the TST, a mouse, suspended by the tail for a short period of time, shows alternate periods of agitation and immobility called "searching" and "waiting" phases, respectively. The searching phase is characterized by body jerks, running motions, and body torsions where the mouse attempts to catch its tail. The waiting phase is characterized by the absence of initiated motions and includes passive swaying (immobility). Antidepressants of various types reliably produce a decrease in immobility time relative to saline.

Mice were allowed to adapt to the room and to a white noise generator (to block ambient noises from the surrounding areas) for at least 2 h prior to testing; tests were conducted between 1000 and 1500 h. Mice, naive to the test apparatus, were suspended ~1.5 cm from the tip of their tail with industrial grade duct tape to a bar 60 cm above a flat bench. The experimenter/rater was unaware of the experimental conditions (drug, drug dose) for individual animals. A random number table was used to determine the order in which drugs were administered (Winer 1962). Mice were treated with either saline, a standard dose of imipramine (20 mg/kg) and fluoxetine (20 mg/kg), or A7CDQ (0.01, 0.1, 0.3, 1.0, 3.0, 30 mg/kg) with a 30-min pre-injection time for all. Drug doses and pre-injection times for the standard agents were identical with what has been previously reported (Jacobsen et al. 2008; Ramamoorthy et al. 2008). Mice were tested only once and each dose of test agent was studied in 8–11 mice ($n = 8–11$ mice/treatment). The 6-min suspension test was captured by video recording either with a Logitech QuickCam Pro for notebooks or Nikon Coolpix S210 and Pinnacle USB video capture device or a Canon Rebel T3i. Immobility time for each mouse was determined by viewing each mouse's 6-min trial and recording of the immobility time; each trial was reviewed and scored in triplicate and the mean of the three scores was used. A mouse was considered immobile when it made no active escape movements but included passive swaying. A mouse was considered mobile when making running motions, body jerks, or attempting to catch its tail.

Locomotor-activity assay Mice were allowed to adapt to the test room for at least 1 h prior to testing; tests were conducted between 0800 and 1630 h. Mice, naive to the test apparatus, were placed in individual TruScan Activity System (Coulbourn Instruments, Allentown, PA) photocell arena chambers (model E63-10; 26 cm × 26 cm × 39 cm). Walls of the chamber were transparent and surrounded by two rings of infrared photodetectors (model E63-12). Each ring contained an array of 16 × 16 infrared detectors (spaced 1.524 cm (0.6 in) apart). These rings were interfaced to a computer for monitoring coordinates of the mouse's location. A random-number table was used to determine the order in which drugs were administered (Eswar et al. 2007). Mice were treated with saline or A7CDQ (0.3 mg/kg) with a 0-min pre-injection time. Mice were tested only once, and each dose of test agent was studied in 12–13 mice ($n = 12–13$ mice/treatment). The behavioral analysis examined movement time (s) and movement distance (cm).

Statistical analysis Data for immobility times and for each measure of locomotor activity were analyzed statistically by a one-way analysis of variance (ANOVA) followed by either a Dunnett's t test or Newman-Keuls post hoc comparison test using GraphPad Prism (GraphPad Software Inc. La Jolla, CA). Values of $P < 0.05$ were considered significant.

In vitro uptake-1 (SERT and NET) functional studies

Expression of hSERT in *Xenopus laevis* oocytes Oocytes were harvested and prepared from adult *Xenopus laevis* females following standard procedures (Iwamoto et al., 2006). Stage V–VI oocytes were selected for cRNA injection within 24 h of isolation. cRNA was transcribed from the pOTV vector using a mMessage Machine T7 kit (Ambion Inc., Austin, TX). Oocytes were injected with 32.2 ng of hSERT cRNA (Nanoject Auto Oocyte Injector, Drummond Scientific Co., Broomall, PA) and incubated at 18 °C for 4–12 days in Ringer's solution supplemented with sodium pyruvate (550 μg/mL), streptomycin (100 μg/mL), tetracycline (50 μg/mL), and 5% dialyzed horse serum.

Primary sequences of mouse and human monoamine transporters are extremely similar (92.8% identity hSERT vs mSERT; 94.2% identity hNET vs mNET using Clustal Omega). The few differences between species comprise helices in the structure that are not within the putative primary site of drug-transporter interaction depicted in crystal structures of monoamine transporters. Overall, most importantly, relevant ligands of monoamine transporters showed comparable potencies to produce effects at murine and human transporters (Han and Gu 2006). Although subtle, differences of ligand effects might be observed at mouse vs human transporters, using the human counterpart has invaluable translational value that justifies its use.

Electrophysiology/two-electrode voltage clamp We performed two-electrode voltage-clamp (TEVC) experiments as previously described (Rodriguez-Menchaca et al. 2012). Electrodes having resistances from 1 to 5 MΩ were filled with 3 M KCl. *Xenopus laevis* oocytes expressing hSERT were voltage-clamped to − 60 mV with a GeneClamp 500 (Axon Instruments), and the holding currents were recorded using Clampex 10 (Axon Instruments). Extracellular buffer consisted of (in mM) the following: 120 NaCl, 7.5 HEPES, 5.4 K gluconate, 1.2 Ca gluconate, pH 7.4. Recordings were

done at room temperature (23–25 °C). In a typical recording, extracellular buffer was perfused until stable baseline currents were obtained, and then experimental compounds were perfused (duration of compound perfusion is indicated in the figures by solid horizontal lines over the traces).

Analysis To control for transporter expression among oocytes, we normalized each drug-induced trace obtained in individual hSERT-expressing oocytes to a 5 μM 5-HT-induced current (recorded prior to application of each compound tested). Values for peak current amplitudes from drug-induced responses were selected at 10–20 s for all drug concentrations and normalized to the 5-HT-induced response. To obtain concentration-response curves for hSERT-induced peak currents, normalized values for all drug concentrations were averaged from several oocyte recordings and fitted to the Hill 1 equation, $y = Vmax + (Vmin - Vmax) * xn/(kn + xn)$, which yielded K_m and Vmax values, using Origin 8.0, (OriginLab Corporation, Northampton, MA). The dose-response curves and statistics were determined with GraphPad Prism (GraphPad Software Inc. La Jolla, CA).

Intracellular Ca^{+2} determinations Intracellular Ca^{2+} concertation was measured, as previously described, in cells permanently expressing NET and transfected with voltage-gated Ca^{2+} channel, $Ca_V1.2$ (Solis et al. 2017). Briefly, stable cell lines expressing NET were developed using the Flp In-TREx system (Invitrogen). Cells were plated in 96-well flat-bottom imaging plates, then were co-transfected with plasmids coding α1, β3, α2δ, and EGFP in a ratio (1.2:0.5:1:0.2, in μg) using Fugene 6 as transfecting reagent. The culturing media were supplemented with doxycycline (1 μg/mL) 3 days before the experiment to induce expression of the monoamine transporter.

Fura-2 was used as intracellular Ca^{2+} sensor; experiments were carried out under constant perfusion at 35 °C (ThermoClamp-1, Automate Scientific) in an Olympus IX70 microscope equipped with 20× 0.75NA objective and a fluorescence imaging attachment (Till Photonics). Ratio images (340 nm and 380 nm excitation) were acquired at 3 Hz and recoded for off-line analysis. As previously described, experiments were done using Imaging Solution (IS) consisting of: 130 NaCl, 4 KCl, 2 CaCl2, 1 MgCl2, 10 Hepes, 10 glucose (in mM), pH 7.3. (Ruchala et al. 2014, Cameron et al. 2015). DA is a very strong substrate at NET, this is not surprising giving its structural similarity to NE (Rothman and Baumann, 2003), and it was used as positive control in NET experiments. A7CDQ, that worked as substrate, was subjected to the following protocol: cells were first perfused for 10 s with IS and then exposed to DA 10 μM as a positive control for 5 s; after 30 s IS wash, cells were exposed to A7CDQ at a given concentration for 5 s and then to a final IS wash for an additional 30 s. For A6CDQ that worked as an inhibitor, cells were

perfused for 10 s with IS, then exposed to DA 10 μM for 5 s, followed by an IS wash for 30 s, then A6CDQ at a given concentration was perfused for 15 s and then exposed A6CDQ plus DA 10 μM for additional 5 s, and then cells underwent a final wash of 30 s. Each well was exposed to a single concertation of test agent. The analysis of recorded images was performed using Till Photonics off-line analysis software. The fluorescence intensity of individual cells, normally 5 to 10 cells per well, that responded to the positive control is quantified and saved as a temporal numeric series.

For each dose-response determination, 2–5 wells were collected per dose, normally 2 to 3 different sets of experiments were used to collect data; thus, each concentration point has data of at least 4 wells (> than 20 cells). The amplitude of the signal produced by A7CDQ or the amplitude of the signal of DA 10 μM in the presence A6CDQ is divided by the signal produced by the positive control (DA 10 μM) for each individual cell. This ratio was used to generate a dose-response curve using Prism 5.0 software as described previously (Solis et al. 2017).

APP^+ uptake 4-(4-Dimethylamino)phenyl)-1-(methylpyridinium (APP^+), a fluorescent substrate of mono-amine transporters, was used to monitor the activity of NET in cells (cells are described above). Cells expressing NET were plated in 96-well flat-bottom imaging plates, and NET expression was induced with doxycycline (1 μg/mL) 3 days before experiments. Cells were placed in the stage of a fluorescence microscope, and APP^+ was detected using an excitation light of 460/10 nm and emission light of 535/50 nm. Experiments were performed under constant perfusion at room temperature. Cells were exposed to IS (see composition above) for 10 s, then to 30 s of the test drug at a given concentration, and then to test drug plus APP^+ 3 μM. For each experiment, few wells were tested in the absence of test drug (only APP^+ 3 μM) as control. The APP^+ signal of each cell in a well was quantified, and the first derivative of the curve was computed using Prism 5.0 to get the rate of APP^+ uptake. The maximal uptake of APP^+ of each cell in a well was averaged, and that average was expressed as a percentage of the maximal rate of the control wells (without drug). Then, a dose-response curve was generated using Prism 5.0 software for at least 4 experiments.

In vitro uptake-2 (OCT1–3) functional studies

Cell culture and in vitro hOCT kinetic assay Maintenance culture conditions for established human embryonic kidney (HEK)-hOCT1, -hOCT2, and -hOCT3 stably expressing cell lines, and HEK empty vector background control, were as previously published (37 °C; 5% CO_2; DMEM high glucose; 10% serum; 1% Pen/Strep; 600 μg/ml G418) (Mulgaonkar et al. 2013; Pan et al. 2013). Basic assay conditions, including MPP^+ concentration and uptake time used for kinetic

analyses, were as previously reported (Pan et al. 2017). Specifically, cells (2×10^5 cells/well) were seeded into wells (24-well tissue culture plate) and grown for 48 h without antibiotics. Prior to uptake assay, cells were equilibrated with transport buffer (10 min; 500 μL of Hanks' balanced salt solution containing 10 mM HEPEs, pH 7.4). This solution was replaced with 500 μL of fresh transport buffer containing 1 μM unlabeled 1-methyl-4-phenylpyridinium (MPP^+) spiked with [H^3]MPP^+ (0.25 μCi/mL) in the absence or presence of test compounds (10^{-8} to 10^{-4} M A6CDQ or A7CDQ). Post incubation, experimental media were removed, and the cells were washed three times with ice-cold transport buffer. Cells were then lysed (200 μL of 1 M NaOH) and subsequently neutralized (250 μL of 1 M HCl plus 200 μL of 0.1 M HEPES). Radioactivity was quantified by liquid scintillation counting, and uptake profiles were normalized by total protein content determined by the Bradford method. Intracellular accumulation of MPP^+ was calculated as picomoles of substrate per milligram total protein after correction for background accumulation in empty vector transfected control cells and is reported as percent of control. The half-maximal inhibitory concentrations (IC_{50}) were calculated using nonlinear regression and the "log (inhibitor) versus response" model (GraphPad Prism Software version 6.0; GraphPad Software Inc., San Diego, CA). Results were confirmed by repeating all experiments at least three times with triplicate wells for each data point in every experiment.

Results

A7CDQ is a 5-HT$_3$ receptor competitive antagonist

In electrophysiological studies, A7CDQ failed to induce currents from *Xenopus laevis* oocytes expressing m5-HT$_3$A receptors when applied alone. When co-applied with 2.2 μM 5-HT, A7CDQ inhibited 5-HT-induced responses with an $IC_{50} = 5.77 \pm 1.13$ μM (nH $= -2.09$; $n = 4$; Fig. 2).

A7CDQ shows antidepressant-like effect in the mouse TST

A7CDQ was examined for antidepressant-like action in the mouse TST assay at doses ranging from 0.01 to 30 mg/kg and exhibited statistically lowered immobility times at a 1.0 mg/kg dose when compared to saline ($F = 6.338$; df $= 74$; $P < 0.05$; Dunnett's post hoc test $P < 0.05$, 1.0 mg/kg dose; Fig. 3).

The reduction in immobilization time produced by A7CDQ (1.0 mg/kg) is comparable to the effect for the tricyclic antidepressant imipramine (20 mg/kg), the SSRI fluoxetine (20 mg/kg), and A6CDQ (1.0 mg/kg) and significantly different from saline (0.9% 10 mL/kg)-treated control (Fig. 4).

A7CDQ does not exert locomotor stimulant or depressant effects

An effective TST dose of A7CDQ, 1.0 mg/kg, was tested against saline for hyperactivity in a mouse locomotor activity assay. A7CDQ was injected i.p. and its effect on locomotor activity was examined over 45 min post injection; this time interval encompasses all time required to perform the TST assay described previously (Dukat et al. 2013). Total movement time ($t = 0.2608$, df $= 16$, $P = 0.7976$) and distance ($t = 0.4998$, df $= 15$, $P = 0.6245$) were not significantly different between A7CDQ and the saline control (t test) (Fig. 5).

A6CDQ and A7CDQ are substrates and/or inhibitors of uptake-1

We recorded currents from oocytes expressing hSERT in response to 5-HT, fluoxetine, A6CDQ, and A7CDQ. The endogenous hSERT substrate 5-HT (5 μM) induced an inward current distinctive for substrates (Fig. 6a–c). Fluoxetine, a hSERT blocker, produced an outward deflection in the current trace indicative of the blockade of a SERT-mediated constitutive "leak" current (Fig. 6c). A6CDQ (10 μM) induced an inward current with a smaller amplitude compared to the 5-HT response (Fig. 6a). Conversely, as did fluoxetine, A7CDQ (100 μM) induced outward currents that are attributed to blockade of the hSERT constitutive leak (Fig. 6b and c, respectively). Concentration-response curves for inducing inward-hSERT currents yielded an $EC_{50} = 0.94$ μM for 5-HT and comparable potency for A6CDQ ($EC_{50} = 2.80$ μM). The potency for inducing outward hSERT currents was much stronger for fluoxetine than for A7CDQ ($EC_{50} = 0.076$ μM and 43.6 μM, respectively) (Fig. 6d).

Compounds that are ligands at NET interfere with APP^+ uptake and can be evaluated in real time using fluorescence microscopy in HEK293 cells expressing NET. Dopamine (DA) is a strong substrate at NET and inhibits APP^+ maximal uptake rate ($IC_{50} = 0.09 \pm 0.01$ μM); A6CDQ and A7CDQ were much weaker than DA at inhibiting APP^+ maximal uptake rate showing IC_{50} values of 1.34 ± 0.25 and 2.39 ± 0.50 μM, respectively (Fig. 7).

A permanent cell line that expresses hNET was transfected with the voltage-gated Ca^{2+} channel Ca$_V$1.2, and intracellular Ca^{2+} signals were measured using Fura-2 in an epifluorescence microscope. The application of DA 10 μM for 5 s induced a reproducible Ca^{2+} signal that returned to baseline within a 30-s wash; A7CDQ produced a Ca^{2+} signal less efficacious than DA and showed an EC_{50} of 3.3 ± 0.4 μM (Fig. 8). On the other hand, A6CDQ produced a nearly undetectable signal when applied alone but competed with a 10 μM DA-induced signal with an IC_{50} of 1.8 ± 0.4 μM (Fig. 8).

A6CDQ and A7CDQ are inhibitors of uptake-2

The inhibitory effects of A6CDQ and A7CDQ were examined at three OCT paralogs, hOCT1, hOCT2, and hOCT3, using the prototypical hOCT substrate MPP^+. Significant accumulation of MPP^+ was observed in stably transfected hOCT-expressing HEK293 cells (always greater than 10-fold) relative to empty vector transfected background control HEK293 cells
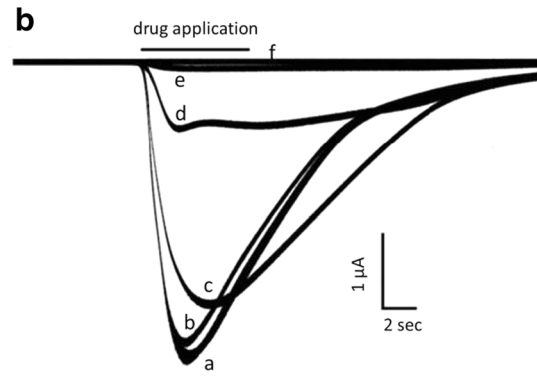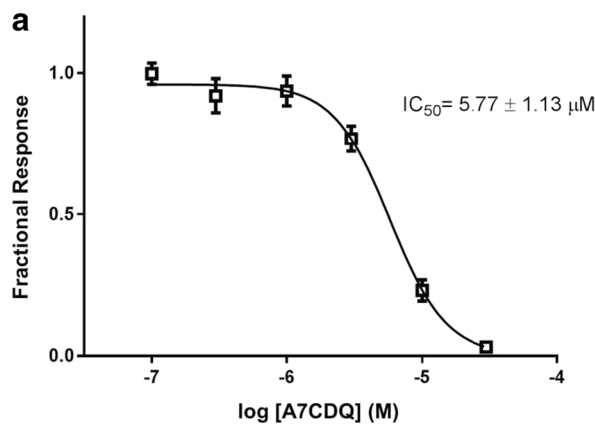
Fig. 2 Inhibition of 5-HT-induced currents by A7CDQ. (**A**) A7CDQ reduced peak currents with an $IC_{50} = 5.77 \pm 1.13$ μM with a Hill slope (nH) $= -2.09$. (**B**) Inhibition of m5-HT$_3$A responses to 2.2 μM 5-HT by

A7CDQ. A7CDQ concentrations: a $= 0.1$ μM, b $= 0.3$ μM, c $= 1.0$ μM, d $= 3.0$ μM, e $= 10$ μM, f $= 30$ μM

(background $= \sim 1$–3 pmol/mg protein/1 min). Concentration-response (10^{-8} to 10^{-4} M A6CDQ or A7CDQ) studies were performed to derive IC_{50} values for each compound on hOCT1–3. IC_{50} values for A6CDQ at hOCT1–3 were estimated as 3.0, 16.4, and 3.9 μM, respectively (Fig. 9 and Table 2). The IC_{50} values for A7CDQ at hOCT1–3 were estimated as 4.8, 9.2, and 5.9 μM, respectively (Fig. 9 and Table 2).

Discussion

There are several possible mechanisms that might underlie the observed antidepressant-like effect of A6CDQ in the TST. One distinctive property of A6CDQ is its potent action on
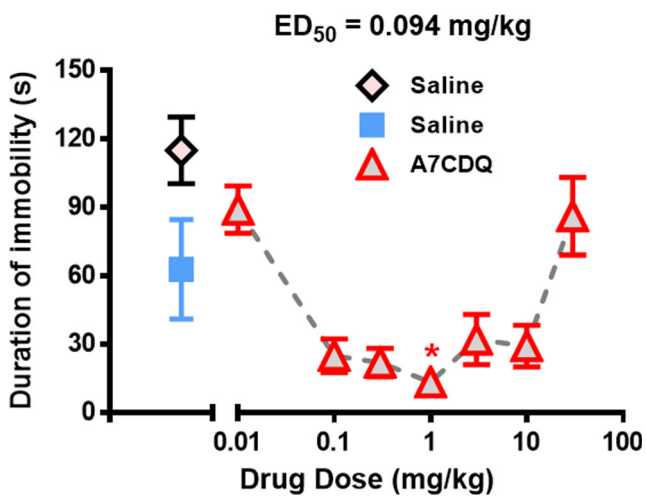
5HT$_3$ receptors in binding and functional studies (Dukat et al. 2013). Direct or indirect inhibition of 5HT$_3$ receptors by commonly used antidepressants, such as fluoxetine, implicates 5HT$_3$ receptors as a therapeutic target for depression treatment (Andersen et al. 2014; Eisensamer et al. 2003); thus, we proposed that A6CDQ antidepressant activity relied on its antagonistic activity at 5-HT$_3$ receptors (Dukat et al. 2013). To further examine the role of 5-HT$_3$ receptors in the actions of A6CDQ, we studied a positional isomer, A7CDQ, that binds with substantially lower affinity than A6CDQ at 5-HT$_3$

Fig. 3 Effect ($\pm$S.E.M.) of acute administration of A7CDQ (i.p.) on duration of immobility in the mouse TST ($n = 8$–11 mice/treatment). Black diamond saline corresponds only to the 0.01 mg/kg dose of A7CDQ, whereas the blue square saline represents control for all other drug doses. Asterisk denotes a significant difference compared to control group (square symbol; 0.9% saline; 10 mL/kg); *$P < 0.05$; one way ANOVA ($F = 6.338$; df $= 74$; $P = 0,006$) followed by Dunnett's multiple comparison test $P < 0.05$
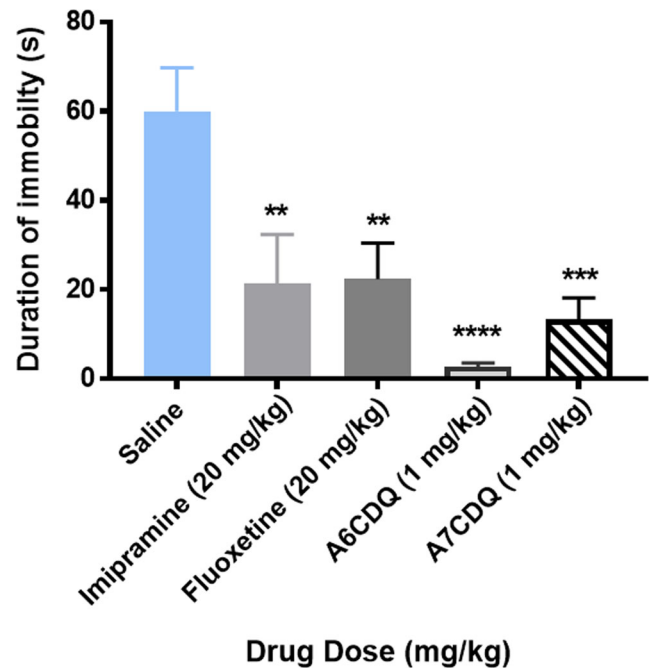

Fig. 4 Effect ($\pm$SEM) of acute administration of standard doses of clinically employed antidepressants (imipramine and fluoxetine) and A6CDQ and A7CDQ (i.p.) on duration of immobility in the mouse TST ($n = 8$–11 mice/treatment). Asterisk denotes a significant difference compared to control group (0.9% saline; 10 mL/kg); **$P < 0.01$, ***$P < 0.001$, ****$P < 0.0001$ one way ANOVA ($F = 8.23$; df $= 4.52$; $P < 0.0001$) followed by Dunnett's multiple comparison test $P < 0.05$
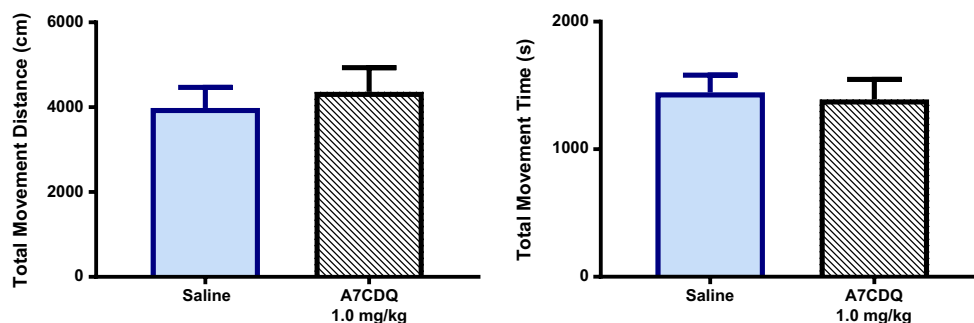
Fig. 5 A7CDQ produced saline-like effects on mouse locomotor activity at an effective TST-active dose. Effect (± SEM) of A7CDQ (1.0 mg/kg; i.p.) on total movement distance (right panel) and total movement time (left panel) relative to 0.9% saline (10 mL/kg; i.p.) ($n = 8$–9 mice per treatment). Unpaired two-tailed t test for total movement distance (cm), A7CDQ $t(15) = 0.4998$, $P = 0.6245$ and for total movement time (s), A7CDQ $t(16) = 0.2608$, $P = 0.7976$

receptors (Dukat et al. 2013). Being positional isomers, the two compounds should share certain physicochemical properties (e.g., lipophilicity) and could highlight the relevance of 5-HT_3 receptor involvement in the TST, that is, if A7CDQ is a 5-HT_3 receptor antagonist, the lower-affinity A7CDQ should be less potent (or inactive) compared to A6CDQ in the mouse TST. Hence, we examined whether or not A7CDQ is a 5-HT_3 receptor antagonist, and whether or not it is active in the mouse TST.

Receptor binding studies indicated that A7CDQ binds competitively at mouse receptors with an affinity ($K_i = 1975$ nM) comparable to its antagonist potency ($IC_{50} = 5.77$ μM) determined in the functional assay. The Hill slope of ~ 2 is consistent with the presence of at least two cooperative ligand-binding sites on the receptor. Given the homopentameric structure of the receptor, it is possible the antagonist binds to all 5 available binding sites. Hence, moving the chloro substituent from the 6- to 7- position of the quinazoline ring (Fig. 1) yielded a positional isomer with 25-fold reduced 5-HT_3 receptor affinity, but retention of antagonist action (Fig. 2) at 5-HT_3 receptors.

We previously demonstrated that A6CDQ is active in the TST assay and hypothesized that this might be related to its action as a 5-HT_3 receptor antagonist (Dukat et al. 2013). Because A7CDQ retains antagonist action at 5-HT_3 receptors, and 5-HT_3 antagonists are active in the TST, our results showed that A7CDQ, despite its lower affinity and potency at 5-HT_3 receptors, produces antidepressant-like effects in the mouse TST (Fig. 3) with comparable potency and efficacy as A6CDQ (Fig. 4).

The TST is only indicative of antidepressant-like activity if the tested drug does not show a stimulant effect. Locomotor stimulants generally increase movement time and distance in mouse locomotor activity assays (Young and Glennon 2008). Similar to what we described for A6CDQ (Dukat et al. 2013), A7CDQ was neither a locomotor stimulant nor a locomotor depressant at the most effective TST dose (Fig. 5).

It was surprising that A7CDQ, a positional isomer of A6CDQ, which has decreased affinity for, and decreased potency as an antagonist at 5-HT_3 receptors, retained the potency of A6CDQ in the TST. Since the two compounds are almost identical and should share similar pharmacokinetic properties,
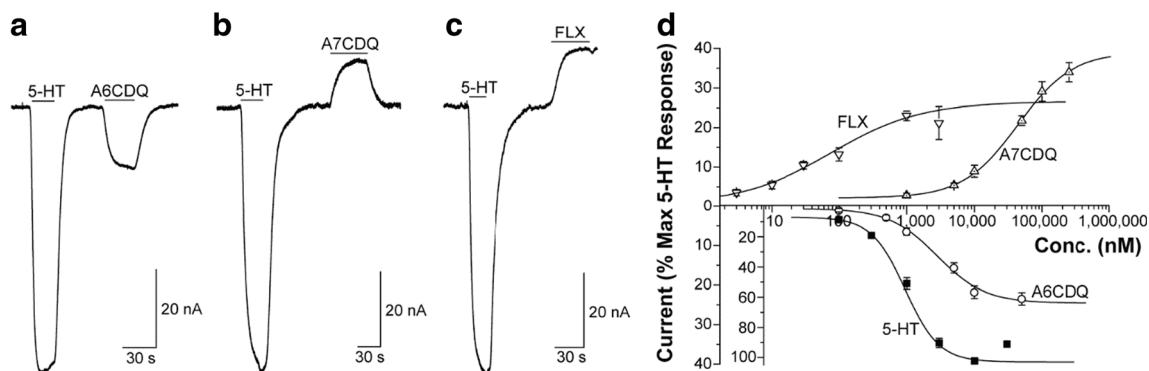

Fig. 6 The electrophysiological signature elicited by A6CDQ, A7CDQ, and fluoxetine (FLX) on hSERT in hSERT-expressing oocytes voltage-clamped to − 60 mV. The concentrations for the representative recordings are 5 μM for 5-HT (panels A–C), 10 μM for A6CDQ (**A**), 100 μM for A7CDQ (**B**), and 1 μM for FLX (**C**). **D** Concentration-response plots for currents induced by 5-HT, FLX, A6CDQ, and A7CDQ. Values are plotted in the direction of the current each compound elicits as a percentage of the maximal 5-HT-induced hSERT current. The y-axis from 0 to +100 corresponds only to the 5-HT concentration-response plot, whereas the y-axis from 0 to +40 corresponds to FLX, A6CDQ, and A7CDQ
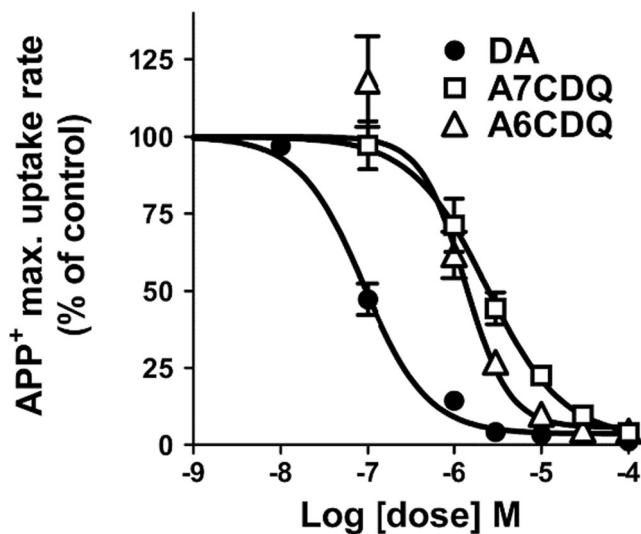
Fig. 7 A7CDQ and A6CDQ inhibit APP^+ uptake in HEK cells expressing hNET. Competition of APP^+ uptake is used to study dopamine (filled circle), A7CDQ (open square), and A6CDQ (open triangle) interaction with hNET. Cells expressing hNET are exposed to APP^+ (3 μM) in the presence of the indicated drugs at different concentrations, and APP^+ uptake is measured by epifluorescence microscopy. The maximal rate of uptake for each concertation is plotted as percentage of the maximal uptake in absence of competing drug (APP^+ alone). Each point is mean ± SEM of 4 experiments, and fitted IC_{50} are 0.09 ± 0.01, 2.39 ± 0.50, and 1.34 ± 0.25 μM for DA, A7CDQ, and A6CDQ respectively

Fig. 9 Inhibitory potency determination. Representative experiments showing 1 min uptake of MPP^+ (1 μM) measured in HEK293 cells stably expressing hOCT3 in the presence of increasing concentrations of unlabeled A6CDQ or A7CDQ (10^{-8} to 10^{-4} M). Data ($n = 3$ per condition) were corrected for nonspecific background measured in empty vector control cells and are shown as mean ± SD. IC_{50} values were determined with nonlinear regression and are reported in Table 2. Identical conditions were used to quantify inhibition potency of these compounds on hOCT1 and hOCT2 as well (Table 2)

these results strongly suggest that targets other than 5-HT$_3$ receptors must be in play to produce the antidepressant-like activity of these 2-aminoquinazoline derivatives observed in the TST. TST data suggest that the compounds are centrally acting. In addition, using an HPLC method, we determined actual log$P$ values for A6CDQ (log$P = 1.86$; Dukat et al. 2013) and A7CDQ (log$P = 1.93$; Alix 2009). These values fall within the range of log$P$ values for BBB permeant molecules and are in agreement with Hansch's (Hansch et al. 1987)
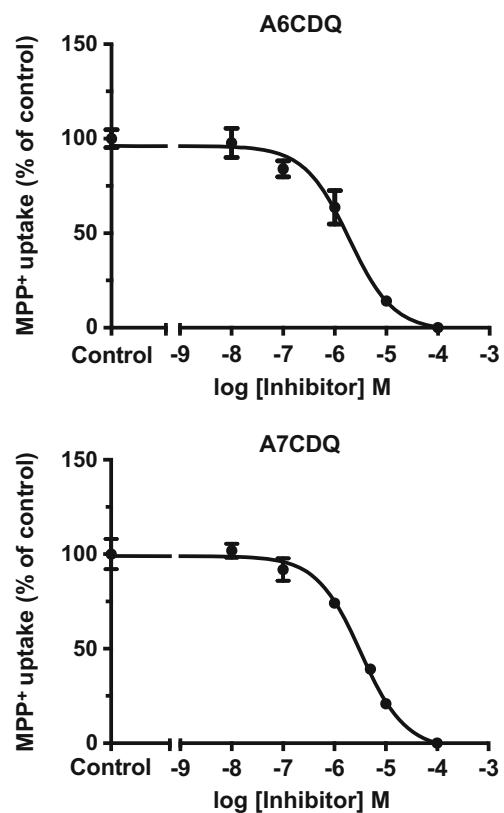
postulate that drugs with log$P$ values in the range of 1.5 to 2.5 will, in general, "find ready entry into the brain ...". In
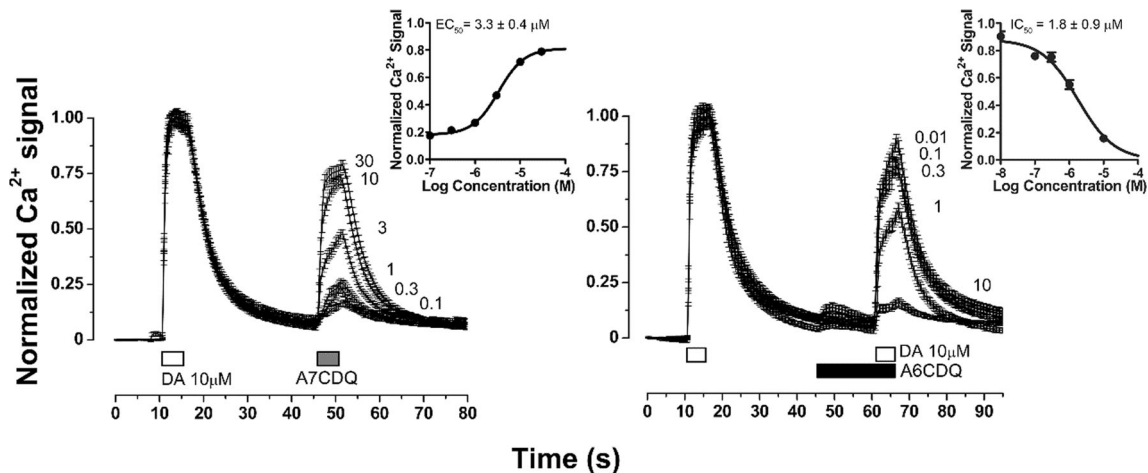

Fig. 8 A7CDQ is a substrate and A6CDQ is a blocker of hNET. HEK cells expressing hNET were transfected with the voltage-gated Ca^{2+} channel ($Ca_V1.2$), loaded with Fura-2 and the intracellular Ca^{2+} signals were measured using epifluorescence microscopy. Dopamine is a substrate in hNET

that produce a Ca^{2+} signal (positive control). A7CDQ produce Ca^{2+} signals in a dose-dependent manner (left panel). A6CDQ shows a very weak signal when applied alone and it can block the Ca^{2+} signal induced by DA 10 μM in a dose-dependent manner (right panel)

Table 2 Half-maximal inhibitory (IC_{50}) concentrations ($\mu M \pm SD$) at hOCTs (vs MPP^+)

Ligands	hOCT1	hOCT2	hOCT3
A6CDQ	3.0 ± 0.8	16.4 ± 4.7	3.9 ± 2.4
A7CDQ	4.8 ± 1.2	9.2 ± 2.8	5.9 ± 3.9

addition, both analogs comply with Lipinski's (Lipinski 2004) rules for CNS penetration suggesting they should readily penetrate the BBB. Yet, another indicator for CNS drugs that penetrate the BBB is total polar surface area (TPSA) < 70 Å^2 (Kelder et al. 1999) and our compounds that meet this requirement with TPSA = 50.41 Å^2 (www.molinspiration.com). These findings suggest that both compounds are brain penetrant, and that any pharmacological differences are unlikely to be ascribed to their difference to penetrate the BBB.

To gain a better understanding of the pharmacodynamic properties of A6CDQ and A7CDQ that would give rise to their antidepressant-like activity, we performed experiments designed to measure their action on monoaminergic uptake-1 and uptake-2 mechanisms.

It is well accepted that substrates of monoamine transporters, although displaying much lower potencies for monoamine transporters than inhibitors (in uptake competition assays), have significant effects as releasing agents (Rothman and Baumann, 2003). Although neither A6CDQ nor A7CDQ displayed high affinity for SERT ($K_i > 10, 000$ nM), we examined their effect in hSERT-expressing oocytes, a technique that can discriminate substrates from blockers. Our results suggest that A6CDQ and A7CDQ work as a substrate and weak inhibitor in hSERT (Fig. 6), respectively. Substrates of monoamine transporters in addition to competing with endogenous neurotransmitter reuptake, can produce further release of the neurotransmitter in vivo promoting a larger increase of extracellular neurotransmitter than inhibitors (Nash and Brodkin, 1991; Kuczenski et al. 1991; Gudelsky and Nash, 1996). These results suggest that A6CDQ will have a stronger effect than A7CDQ, increasing the extracellular concentration of 5-HT as a result of SERT interaction.

Another possible target that can be involved in the antidepressant activity of A6CDQ and A7CDQ is NET. APP^+, an analog of MPP^+, is a strong substrate at NET that becomes fluorescent when it is internalized and interacts with intracellular components (Solis et al. 2012). Although the inhibition of APP^+ uptake can identify a ligand at NET, it cannot distinguish between substrates and inhibitors of this transporter. Electrophysiological measurements of monoamine transporters have been widely used to study and identify substrates and inhibitors on these transporters; as we mentioned above, substrates produce inward currents that depolarize the plasma membrane when they interact with transporters, and inhibitors inhibit a constitutive leak current (Fig. 6). As we showed for

hSERT, it is possible to express this transporter in oocytes and measure these currents directly using a two-electrode voltage clamp procedure (Fig. 6); unfortunately, hNET does not express in oocytes and this type of recording is not possible. Thus, we used a recently validated method to measure the electrical properties of compounds that interact with monoamine transporters (Solis et al. 2017; Battisti et al. 2018). This method consists of co-expressing a monoamine transporter and a voltage-gated Ca^{2+} channel in HEK cells; substrates activate transporter-mediated currents that depolarize the plasma membrane and open voltage-gated Ca^{2+} channels, resulting in a measurable Ca^{2+} signal (Ruchala et al. 2014; Cameron et al. 2015). In these experiments, arbitrarily, we use as positive control DA at NET. DA and NE both are synthesized from tyrosine and structurally are catecholamines. Interestingly, DA is a very strong substrate showing almost identical pharmacological uptake and release effects as NE at NET in rat brain synaptosome preparations (Rothman and Baumann 2003). In addition, most if not all strong substrates at DAT, such as amphetamine, methamphetamine, and 3,4-methylenedioxymethamphetamine (MDMA) among others, are also very potent substrates at NET (Rothman and Baumann 2003). Physiologically, it is believed that in the pre-frontal cortex, DA is taken up by NET-containing terminals, and the therapeutic action of NET-selective reuptake inhibitors would be mediated by NET blockade in this area (Arnsten 2009; Bymaster et al. 2002). Since NET shows no preference between DA or NE, either can be used as a positive control when tested in vitro with no noticeable differences for selecting one over the other. Our results suggest that, like DA, A7CDQ is a substrate, whereas A6CDQ is an inhibitor that blocks DA-induced signals at NET (Fig. 8), suggesting that even if the affinity of A7CDQ is low ($K_i > 10,000$ vs 261 nM for A6CDQ), it can have releaser activity at hNET.

Recently, we reported that phenylguanidines (PG) are inhibitors of hOCT3 (Pan et al. 2017). Since A6CDQ and A7CDQ are "constrained" analogs of 4-chloro and 3-chloro PG (OCT3; $IC_{50} = 2.8$ and 7.6 μM, respectively) (Pan et al. 2017), we examined if A6CDQ and A7CDQ retained inhibitory actions at hOCT3, activity that also can contribute to their antidepressant effects. Both A6CDQ and A7CDQ were found to be relatively potent inhibitors of all three hOCT paralogs. The apparent rank order of inhibitory potency was the same for both compounds, hOCT1 $\geq$ hOCT3 > hOCT2. Further, translocation of the chloro group from the 6- to the 7-position did not produce any significant changes in the inhibitory potency (IC_{50}) of either compound towards any of the hOCTs, i.e., the position of the chloro group did not influence compound interaction with hOCT1–3.

Conclusions We have demonstrated that 2-aminodihydroquinazolines represent a novel class of agents with potential antidepressant actions. In particular, the 2-

aminodihydroquinazolines A6CDQ (Dukat et al. 2013) and A7CDQ (present investigation) are quite active in the mouse TST, and are equipotent. In fact, under our assay conditions, both agents are more potent in the TST than the standard SSRI antidepressant fluoxetine. Initially, it was thought that the 2-aminodihydroquinazolines, at least A6CDQ, might be acting through a 5-HT$_3$ receptor antagonist mechanism (Dukat et al. 2013). However, its positional isomer, A7CDQ, though also a 5-HT$_3$ receptor antagonist, with an affinity and potency of about 25-fold lower than A6CDQ, was found equipotent with A6CDQ in the TST. These findings prompted us to investigate alternative mechanisms to account for their similarities in potency in the TST.

We hypothesized that this class of agents might target monoamine transporter uptake-1, uptake-2, or a combination of both as part of their antidepressant-like action. In this study, we characterized the effect of A6CDQ and A7CDQ at human variants of uptake-1 and uptake-2. These transport systems are highly conserved in mammals, and the results provided here at human proteins warrant translational value of our findings. A6CDQ and A7CDQ have differential effects in uptake-1 components: A6CDQ is a SERT-releasing agent but an inhibitor at NET, whereas A7CDQ is a releaser at NET and a blocker at SERT. Although the potencies of these compounds on uptake-1 are moderate to low, these actions on uptake-1 might contribute to some extent to the overall antidepressant effect of A6CDQ and A7CDQ.

In summary, both A6CDQ and A7CDQ display equipotent antidepressant-like action in the mouse TST. However, they might do so via somewhat different actions. It would seem that A6CDQ and A7CDQ in addition to their 5-HT$_3$ antagonist action, display "hybrid" transporter activity characterized by a different molecular mechanism at SERT vs NET. As such, A6CDQ is a substrate at SERT but an inhibitor at NET whereas A7CDQ is a substrate at NET but an inhibitor at SERT. In addition, both analogs inhibit OCT3 with similar potency to other strong uptake-2 inhibitors, e.g., decynium-22 or corticosterone (Hayer-Zillgen et al. 2002) and OCT3 has been suggested to represent a component of uptake-2 (Daws et al. 2013). Thus, A6CDQ and A7CDQ might represent the first members of a new class of potential antidepressants with a unique multi-modal mechanism of action: uptake-1 substrates/inhibitors, uptake-2 inhibitors and 5-HT$_3$ receptor antagonists.

We understand the limitations of our preliminary findings using only an acute model of antidepressant-like action, the mouse TST. To expand our understanding of the antidepressant-like action of A6CDQ and A7CDQ, further studies will be required; the ligands will be examined in the chronic mild stress (CMS) model or mouse psychosocial stress model. Eventually, optimized analogs will be examined in SERT/NET/OCT knockout mice to confirm their lack or their significant role in the antidepressant-like action of 2-aminodihydroquinazolines.

The current findings also have some other significant ramifications. It can no longer be assumed that moving a substituent from one position to another, resulting in a common effect, implies a commonality of mechanism. As demonstrated here, the simple translocation of a chloro group, from the 6- to the 7-position of a 2-aminodihydroquinazoline analog (comparing A6CDQ with A7CDQ), results in a common action in a specific in vivo assay (i.e., the TST) but might involve a different mechanism or a combination of different mechanisms.

Compliance with ethical standards Protocols were approved by the Institutional Animal Care and Use Committee (IACUC) of Virginia Commonwealth University.

Conflict of interest The authors declare that they have no conflict of interest.

Publisher's note Springer Nature remains neutral with regard to jurisdictional claims in published maps and institutional affiliations.

References

Alix KE (2009) Novel analogs of m-chlorophenylguanidine as 5-HT$_3$ receptor ligands. Virginia Commonwealth University, Thesis

Andersen J, Stuhr-Hansen N, Zachariassen LG, Koldsø H, Schiøtt B, Strømgaard K, Kristensen AS (2014) Molecular basis for selective serotonin reuptake inhibition by the antidepressant agent fluoxetine (Prozac). Mol Pharmacol 85:703–714

Arnsten AF (2009) Toward a new understanding of attention-deficit hyperactivity disorder pathophysiology: an important role for prefrontal cortex dysfunction. CNS Drugs 23(Suppl 1):33–41

Battisti UM, Sitta R, Harris A, Sakloth F, Walther D, Ruchala I, Negus SS, Baumann MH, Glennon RA, Eltit JM (2018) Effects of N-alkyl-4-methylamphetamine optical isomers on plasma membrane monoamine transporters and abuse-related behavior. ACS Chem Neurosci 9:1829–1839

Bétry C, Etiévant A, Oosterhof C, Ebert B, Sanchez C, Haddjeri N (2011) Role of 5-HT$_3$ receptors in the antidepressant response. Pharmaceuticals 4:603–629

Bymaster FP, Katner JS, Nelson DL, Hemrick-Luecke SK, Threlkeld PG, Heiligenstein JH, Morin SM, Gehlert DR, Perry KW (2002) Atomoxetine increases extracellular levels of norepinephrine and dopamine in prefrontal cortex of rat: a potential mechanism for efficacy in attention deficit/hyperactivity disorder. Neuropsychopharmacology. 27: 699–711

Cameron KN, Solis E Jr, Ruchala I, De Felice LJ, Eltit JM (2015) Amphetamine activates calcium channels through dopamine transporter-mediated depolarization. Cell Calcium 58:457–466

Carlsson A, Corrodi H, Fuxe K, Hökfelt T (1969) Effects of some antidepressant drugs on the depletion of intraneuronal brain catecholamine stores caused by 4, alpha-dimethyl-meta-tyramine. Eur J Pharmacol 5:367–373

Davies PA (2011) Allosteric modulation of the 5-HT$_3$ receptor. Curr Opin Pharmacol 11:75–80

Daws LC, Koek W, Mitchell NC (2013) Revisiting serotonin reuptake inhibitors and the therapeutic potential of "uptake-2" in psychiatric disorders. ACS Chem Neurosci 4:16–21

Dukat M, Alix K, Worsham J, Khatri S, Schulte MK (2013) 2-Amino-6-chloro-3,4-dihydroquinazoline: a novel 5-HT$_3$ receptor antagonist with antidepressant character. Bioorg Med Chem Lett 23:5945–5948

Eisensamer B, Ramme G, Gimpl G, Shapa M, Ferrari U, Hapfelmeier G, Bondy B, Parsons C, Gilling K, Zieglgänsberger W, Holsboer F, Rupprecht R (2003) Antidepressants are functional antagonists at the serotonin type 3 (5-HT$_3$) receptor. Mol Psychiatry 8:994–1007

Eswar N, Webb B, Marti-Renom MA, Madhusudhan MS, Eramian D, Shen M-Y, Pieper U, Sali A (2007) Comparative protein structure modeling using modeler. Curr Protoc Bioinformatics 5(6):1–5.6.30

Gudelsky GA, Nash JF (1996) Carrier-mediated release of serotonin by 3, 4-methylenedioxymethamphetamine: implications for serotonin-dopamine interactions. J Neurochem 66:243–249

Han DD, Gu HH (2006) Comparison of the monoamine transporters from human and mouse in their sensitivities to psychostimulant drugs. BMC Pharmacol 6:6

Hansch C, Bjorkroth JP, Leo A (1987) Hydrophobicity and central nervous system agents: on the principle of minimal hydrophobicity in drug design. J Pharm Sci 76:663–687

Hayer-Zillgen M, Brüss M, Bönisch H (2002) Expression and pharmacological profile of the human organic cation transporters hOCT1, hOCT2 and hOCT3. Br J Pharmacol 136:829–836

Hope AG, Peters JA, Brown AM, Lambert JJ, Blackburn TP (1996) Characterization of a human 5-hydroxytryptamine3 receptor type A (h5-HT3R-AS) subunit stably expressed in HEK 293 cells. Br J Pharmacol 118:1237–1245

Iwamoto H, Blakely RD, De Felice LJ (2006) Na$^+$, Cl$^-$, and pH dependence of the human choline transporter (hCHT) in *Xenopus* oocytes: the proton inactivation hypothesis of hCHT in synaptic vesicles. J Neurosci 26:9851–9859

Jacobsen JPR, Nielsen EØ, Hummel R, Redrobe JP, Mirza N, Weikop P (2008) Insensitivity of NMRI mice to selective serotonin reuptake inhibitors in the tail suspension test can be reversed by co-treatment with 5-hydroxytryptophan. Psychopharmacology 199:137–150

Kelder J, Grootenhuis PD, Bayada DM, Delbressine LP, Ploemen JP (1999) Polar molecular surface as a dominating determinant for oral absorption and brain penetration of drugs. Pharm Res 16:1514–1519

Kuczenski R, Segal DS, Aizenstein ML (1991) Amphetamine, cocaine, and fencamfamine: relationship between locomotor and stereotypy response profiles and caudate and accumbens dopamine dynamics. J Neurosci 11:2703–2712

Lipinski CA (2004) Lead- and drug-like compounds: the rule-of-five revolution. Drug Discov Today Technol 1:337–334

Lucki I, Dalvi A, Mayorga AJ (2001) Sensitivity to the effects of pharmacologically selective antidepressants in different strains of mice. Psychopharmacology 155:315–322

Marona-Lewicka D, Nichols DE (1997) The effect of selective serotonin releasing agents in the chronic mild stress model of depression in rats. Stress 2:91–100

Miyake A, Mochizuki S, Takemoto Y, Akuzawa S (1995) Molecular cloning of human 5-hydroxytryptamine3 receptor: heterogeneity in distribution and function among species. Mol Pharmacol 48:407–416

Mulgaonkar A, Venitz J, Grundemann D, Sweet DH (2013) Human organic cation transporters 1 (SLC22A1), 2 (SLC22A2), and 3 (SLC22A3) as disposition pathways for fluoroquinolone antimicrobials. Antimicrob Agents Chemother 57:2705–2711

Nash JF, Brodkin J (1991) Microdialysis studies on 3,4-methylmethamphetamine-induced dopamine release: effect of dopamine uptake inhibitors. J Pharmcol Exp Ther 259:820–825

Pan X, Wang L, Grundemann D, Sweet DH (2013) Interaction of ethambutol with human organic cation transporters (SLC22 family) indicates potential for drug-drug interactions during antituberculosis therapy. Antimicrob Agents Chemother 57:5053–5059

Pan X, Iyer KA, Liu H, Sweet DH, Dukat M (2017) A new chemotype inhibitor for the human organic cation transporter 3 (hOCT3). Bioorg Med Chem Lett 27:4440–4445

Perez-Palomar B, Mollinedo-Gajate I, Berrocoso E, Meana JJ, Ortega JE (2018) Serotonin 5-HT3 receptor antagonism potentiates the antidepressant activity of citalopram. Neuropharmacology 133:491–502

Porsolt RD, Le Pichon M, Jalfre M (1977) Depression: a new animal model sensitive to antidepressant treatments. Nature 266:730–732

Ramamoorthy R, Radhakrishnan M, Borah M (2008) Antidepressant-like effects of serotonin type-3 antagonist, ondansetron: an investigation in behaviour-based rodent models. Behav Pharmacol 19:29–40

Ramamoorthy R, Radhakrishnan M (2010) The auspicious role of the 5-HT$_3$ receptor in depression: a probable neuronal target? J Psychopharmacol 24:455–469

Rodriguez-Menchaca AA, Solis E Jr, Cameron K, De Felice LJ (2012) S(+)amphetamine induces a persistent leak in the human dopamine transporter: molecular stent hypothesis. Br J Pharmacol 165:2749–2757

Rothman RB, Baumann MH (2002) Therapeutic and adverse actions of serotonin transporter substrates. Pharmacol Ther 95:73–88

Rothman RB, Baumann MH (2003) Monoamine transporters and psychostimulant drugs. Eur J Pharmacol 479:23–40

Ruchala I, Cabra V, Solis E Jr, Glennon RA, De Felice LJ, Eltit JM (2014) Electrical coupling between the human serotonin transporter and voltage-gated Ca(2+) channels. Cell Calcium 56:25–33

Scorza C, Silveira R, Nichols DE, Reyes-Parada M (1999) Effects of 5-HT-releasing agents on the extracellular hippocampal 5-HT of rats. Implications for the development of novel antidepressants with a short onset of action. Neuropharmacology 38:1055–1061

Solis E Jr, Zdravkovic I, Tomlinson ID, Noskov SY, Rosenthal SJ, De Felice LJ (2012) 4-(4-(Dimethylamino)phenyl)-1-methylpyridinium (APP+) is a fluorescent substrate for the human serotonin transporter. J Biol Chem 287:8852–8863

Solis E Jr, Partilla JS, Sakloth F, Ruchala I, Schwienteck KL, De Felice LJ, Eltit JM, Glennon RA, Negus SS, Baumann MH (2017) N-Alkylated analogs of 4-methylamphetamine (4-MA) differentially affect monoamine transporters and abuse liability. Neuropsychopharmacology 42:1950–1961

Steru L, Chermat R, Thierry B, Simon P (1985) The tail suspension test: a new method for screening antidepressants in mice. Psychopharmacology 85:367–370

Thompson AJ, Lummis SC (2013) Discriminating between 5-HT$_3$A and 5-HT$_3$AB receptors. Br J Pharmacol 169:736–747

WHO (2018) Depression http://www.who.int/en/news-room/fact-sheets/detail/depression. Accessed 20 September 2018

Winer BJ (1962) Statistical principles in experimental design. McGraw-Hill, New York

Young R, Glennon RA (2008) MDMA (*N*-methyl-3,4-methylenedioxyamphetamine) and its stereoisomers: similarities and differences in behavioral effects in an automated activity apparatus in mice. Pharmacol Biochem Behav 88:318–331